Available online at www.sciencedirect.com
SCIENCE DIRECT®
European Journal of Pharmaceutics and Biopharmaceutics 64 (2006) 66–74
European Journal of Pharmaceutics and Biopharmaceutics
www.elsevier.com/locate/ejpb

Research paper

# Compaction behaviour and new predictive approach to the compressibility of binary mixtures of pharmaceutical excipients

V. Busignies [a], B. Leclerc [a], P. Porion [b], P. Evesque [c], G. Couarraze [a], P. Tchoreloff [a,*]

[a] *Centre d'études Pharmaceutiques de l'Université Paris XI, France*
[b] *Centre de Recherche sur la Matière Divisée – UMR 6619, CNRS and Université d'Orléans, France*
[c] *Laboratoire de Mécanique: Ecole centrale de Paris, Grande Voie des vignes, France*

Received 24 January 2006; accepted in revised form 22 March 2006
Available online 11 May 2006

**Abstract**

The compressibility of three pharmaceutical excipients (microcrystalline cellulose, lactose and anhydrous calcium phosphate) and their binary mixtures was studied. The aim of this work was to observe the impact of the mass composition of the mixture on the compressibility. The single-compound materials and their mixtures were compacted using instrumented presses. It allowed obtaining compression cycles (i.e., force–displacement curves) which were associated with energy measurements (specific compaction energy, $E_{sp\,cp}$ and specific expansion energy, $E_{sp\,exp}$). It was observed that for the mixtures studied, the change of $E_{sp\,cp}$ with the mass composition could be fitted using a linear relationship (it was not the case with $E_{sp\,exp}$). A linear relationship between the porosity of mixture's compacts and the mass composition was also obtained. Heckel's plots were then obtained for the three excipients and the mixtures. The mean yield pressure was calculated with the ''in-die-method'' and the ''out-of-die method''. A proportional relationship was not valid for the mean yield pressures. But, a predictive approach was proposed in order to obtain indirectly the mean yield pressure of a binary mixture if the data of the single materials were known. It used the linear mixing rule observed with the porosity. The validity was verified and compared with the experimental values. This comparison showed that it was possible to predict the mean yield pressure of binary mixtures from the accessible data of the single excipients.


*Keywords:* Binary mixtures; Compressibility; Porosity; Energetic parameters; Yield pressure; Modelling

## 1. Introduction

Tablets produced in the pharmaceutical industry consist of more than one component. But, if the compaction of mixtures is a common pharmaceutical operation, the mechanisms of their consolidation and their compaction have received little attention when compared with studies performed on single materials. Then, the densification behaviour and the compaction properties are strongly influenced by the characteristics of the mixture like fractions of the components. However, very little is known about interactions between particles of dissimilar materials that cause mixtures to produce tablets with different properties than those produced from single substances. In the literature, there are few papers concerning the compaction behaviour of powder mixtures, and contradictory results were found from the relationship between compaction behaviour and mixture composition [1–8]. In fact, linear and non-linear relationships were observed from the mean yield pressure of the single materials and their proportions in the mixture [5,6]. Then, because of the complexity of compaction, a satisfactory theory enabling prediction of the compressibility of the mixtures does not exist at present.

In this work, we studied the compressibility of binary mixtures of excipients commonly used in pharmaceutical technology. With this aim in view, we used a procedure

* Corresponding author. IFR-141, ''Innovation thérapeutique: du Fondamental au Médicament'', Centre d'études Pharmaceutiques de l'Université Paris XI, 5 rue Jean-Baptiste Clément, 92296 Châtenay-Malabry Cedex, France. Tel.: +33 1 46 83 56 11; fax: +33 1 46 83 58 82.
*E-mail address:* pierre.tchoreloff@cep.u-psud.fr (P. Tchoreloff).

0939-6411/$ - see front matter © 2006 Elsevier B.V. All rights reserved.
doi:10.1016/j.ejpb.2006.03.004

**Nomenclature**

| | |
|---|---|
| $V$ | microcrystalline cellulose, Vivapur 12® |
| $F$ | partly amorphous lactose, Fast Flo® |
| $A$ | anhydrous calcium phosphate, A TAB® |
| VA | Vivapur 12®/A TAB® mixtures |
| VF | Vivapur 12®/Fast Flo® mixtures |
| AF | A TAB®/Fast Flo® mixtures |
| $\varepsilon$ | mean compact porosity |
| $E_{cp}$ | compaction energy (J) |
| $E_{exp}$ | expansion energy (J) |
| $E_{sp\,cp}$ | specific compaction energy (J g$^{-1}$) |
| $E_{sp\,exp}$ | specific expansion energy (J g$^{-1}$) |
| $P_{yA}$ | mean yield pressure obtained from the Heckel plot by ''in-die method'' |
| $P_{yB}$ | mean yield pressure obtained from the Heckel plot by ''out-of-die method'' |
| $P_{ye}$ | $1/P_{ye} = 1/P_{yA} - 1/P_{yB}$ (it characterizes the tendency of a material to recover visco-elastically) |
| $n$ | number of experimental trials used in the calculus of the average values |

described in detail in a previous work [9]. The binary mixtures were compared with the use of compression cycles, energetic parameters, porosity variation and Heckel's model. Finally, a predictive model for the mean yield pressure of binary mixtures was proposed. The values obtained with the model were compared with experimental data for various binary mixtures at different concentrations.

## 2. Materials and methods

### 2.1. Excipients

The materials were a microcrystalline cellulose (Vivapur 12®, 5601210932, JRS, Germany, kindly given by JRS), a partly amorphous lactose (Fast Flo®, 8500042062, Foremost, USA) and an anhydrous calcium phosphate (A TAB®, GW930187, Rhodia, France). These excipients consolidate by different mechanisms, Vivapur 12® (V) by plastic deformation and A TAB® (A) by fragmentation [10,11]. Fast Flo® ($F$) has an intermediate behaviour [12].

The same particle size fractions of each material were used to minimize the possible effect of particle size on consolidation. The 100–180 μm sieve fractions were obtained by sieving on a mechanical sieve shaker (AS 200 digit®, Retsch, Germany). The mean particle sizes in volume were obtained by laser diffraction (Coulter LS 230) in conditions of validity of Frauhofer's theory ($162 \pm 35$ μm for A TAB®, $134 \pm 36$ μm for Fast Flo® and $152 \pm 48$ μm for Vivapur 12®). Before use, the fractions were stored in a closed chamber at $48 \pm 6\%$ of relative humidity for at least 3 days. The apparent particle density of each fraction was determined using an helium pycnometer (Acupyc 1330®, Micromeritics, USA), see Table 1.

### 2.2. Preparation of binary mixtures

The binary mixtures (Vivapur 12®/A TAB®:VA, Vivapur 12®/Fast Flo®:VF and A TAB®/Fast Flo®:AF) were prepared in mass percentage (20/80, 35/65, 50/50, 65/35, 80/20, w/w) with a Turbula mixer (type T2C, Willy A Bachofen, Switzerland) at 50 rpm for 5 min (the degree of filling of a 550 ml vessel was about 50%). The mixtures were labelled with their composition (Table 1). For example, VA36 means a mixture of Vivapur 12® and A TAB® with a respective concentration of 35% and 65% in mass. The apparent particle densities of the binary mixtures were calculated from the values of the mixture components according to their weight proportions in the mixture [13] (Table 1):

$$\frac{100}{d_{\text{part mix}}} = \frac{X_1}{d_{\text{part1}}} + \frac{X_2}{d_{\text{part2}}}, \quad (1)$$

where $d_{\text{part1}}$, $d_{\text{part2}}$ and $d_{\text{part mix}}$ are the apparent particle densities of the single components and their mixtures, respectively, $X_1$ and $X_2$ are the weight fractions of the constituent powders.

Table 1
Apparent particle densities for the single-component powders (experimental values; $n = 3$) and the binary mixtures powders (calculated values using Eq. (1))

| Notation | Powder | Apparent particle density (g cm$^{-3}$) |
|---|---|---|
| $V$ | Microcrystalline cellulose, Vivapur 12® | $1.5402 \pm 0.0005$ |
| $A$ | Anhydrous calcium phosphate, A TAB® | $2.8103 \pm 0.0002$ |
| $F$ | Partly amorphous lactose, Fast Flo® | $1.5309 \pm 0.0001$ |
| VF82 | 80% Vivapur 12® + 20% Fast Flo® (w/w) | 1.5383 |
| VF63 | 65% Vivapur 12® + 35% Fast Flo® (w/w) | 1.5369 |
| VF55 | 50% Vivapur 12® + 50% Fast Flo® (w/w) | 1.5355 |
| VF36 | 35% Vivapur 12® + 65% Fast Flo® (w/w) | 1.5341 |
| VF28 | 20% Vivapur 12® + 80% Fast Flo® (w/w) | 1.5328 |
| VA82 | 80% Vivapur 12® + 20% A TAB® (w/w) | 1.6932 |
| VA63 | 65% Vivapur 12® + 35% A TAB® (w/w) | 1.8296 |
| VA55 | 50% Vivapur 12® + 50% A TAB® (w/w) | 1.9898 |
| VA36 | 35% Vivapur 12® + 65% A TAB® (w/w) | 2.1808 |
| VA28 | 20% Vivapur 12® + 80% A TAB® (w/w) | 2.4124 |
| AF82 | 80% A TAB® + 20% Fast Flo® (w/w) | 2.4078 |
| AF63 | 65% A TAB® + 35% Fast Flo® (w/w) | 2.1743 |
| AF55 | 50% A TAB® + 50% Fast Flo® (w/w) | 1.9821 |
| AF36 | 35% A TAB® + 65% Fast Flo® (w/w) | 1.8211 |
| AF28 | 20% A TAB® + 80% Fast Flo® (w/w) | 1.6842 |

### 2.3. Formation of compacts

Parallelepipedical compacts of single-component powders and binary mixture powders ($40 \times 6$ mm$^2$) were

obtained using an instrumented hydraulic press (Perrier Labotest®, France) at compaction pressures between 4 and 210 MPa to obtain parallelepipedical compact of different porosities. The mass of powders used was the mass necessary to obtain a theoretical thickness of 5 mm for the compacts at zero porosity. No lubricant was used in this compaction procedure.

Cylindrical tablets of single-component powders and binary mixture powders, i.e. powders mixed with 0.5% by weight of magnesium stearate (NF-BP-MF2, Akcros Chemicals v.o.f., Netherlands), were manufactured using an eccentric instrumented Frogerais OA tabletting press. The powders were manually poured into the cylindrical die of 1 $cm^3$ (section of 1 $cm^2$ and height of 1 cm). Tablets of various porosities were produced by varying the compaction pressure between 5 and 280 MPa.

For the two compact geometries, the presses and the methods of compaction were described in more detail in previous paper [9]. After compaction, the compacts were stored for at least three days in a closed chamber at a relative humidity of 48 ± 6%. In order to calculate the mean compact porosity ($\varepsilon$), the compacts were measured (micrometer Digimatic 293®, Mitutuyo, Japan) and exactly weighted (Sartorius BP 2215®, Germany) after compaction and after total elastic recovery.

$$\varepsilon = 1 - \frac{\text{apparent density}}{\text{apparent particle density}}. \quad (2)$$

## 3. Results and discussion

### 3.1. Compression cycles

The cycles were obtained from the data collected during the compaction of the cylindrical compacts. Compression cycles (or force–displacement curves) of the single materials show three steps: the first one corresponds to rearrangement and packing, the second one to fragmentation and/or plastic deformation of the particles and finally, the third stage to instantaneous elastic recovery when the applied pressure is released (closed symbols in Fig. 1). The step of rearrangement is the lowest for Fast Flo® and the most important for Vivapur 12®. Whereas the powder volume used and the compaction pressure are the same (1 $cm^3$ and 280 MPa in Fig. 1), the displacement of the upper punch is important in the case of Vivapur 12® due to an important first step of rearrangement and to the plastic deformation of the particles. The compression cycles obtained with the binary mixtures are shown in Fig. 1 (opened symbols). In all the cases, the compression cycles of the binary mixtures are between those of the single components. The cycles are closer for AF mixtures than for VF and VA mixtures.

### 3.2. Energy measurements

The areas below the curve associated to the compression cycle in the force–displacement plane define the work performed. It can be expressed as energies (J) [9,14]. The area under the compaction phase (between the beginning of the force increase and the maximal punch displacement) corresponds to the compaction energy, $E_{cp}$ (J). This is the energy used for rearrangement, fragmentation and/or ductile deformation of the particle. The expansion energy, $E_{exp}$ (J), corresponds to the energy lost by instantaneous elastic recovery. The integral calculus is made between the maximal displacement and the displacement corresponding to the return of the force to zero. To compare the energetic parameters of the single materials and the binary mixtures, the energies are divided by the mass of powder used [9]. These values are expressed as specific energies in

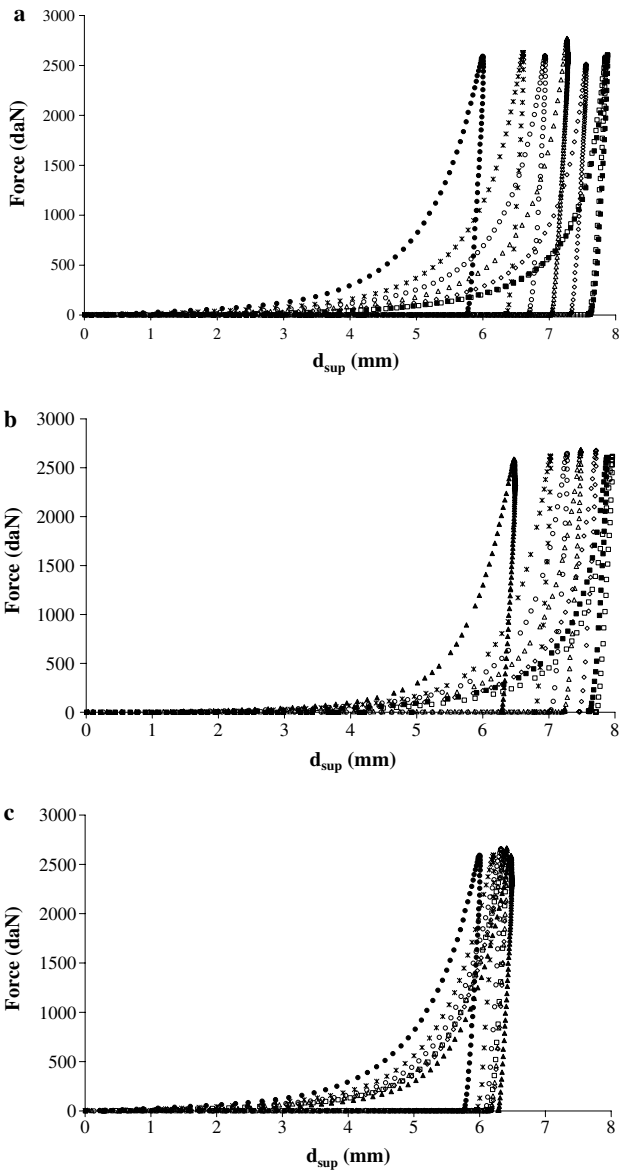


Fig. 1. Compression cycles of binary mixtures for a maximum compaction pressure of 280 MPa. (a) Vivapur 12®/Fast Flo® mixtures (VF), key: ●, F; ■, V; □, VF82; ◇, VF63; △, VF55; ○, VF36; ∗, VF28; (b) Vivapur 12®/A TAB® mixtures (VA), key: ▲, A; ■, V; □, VA82; ◇, VA63; △, VA55; ○, VA36; ∗, VA28; (c) A TAB®/Fast Flo® mixtures (AF), key: ▲, A; ●, F; □, AF82; ◇, AF63; △, AF55; ○, AF36; ∗, AF28.

J $g^{-1}$ ($E_{sp\,cp}$ and $E_{sp\,exp}$). For the single excipients and all the mixtures, the values of the specific energies were obtained for 14 compaction pressures (between 20 and 280 MPa) and for each pressure, 8 trials were realized.

The $E_{sp\,cp}$ and $E_{sp\,exp}$ of the three single materials obtained under various compaction pressures are shown in Figs. 2 and 3. For the range of pressure applied, $E_{sp\,cp}$ is the lowest for A TAB® and intermediate for Fast Flo®. For these two materials, the evolution of $E_{sp\,cp}$ is linear for compaction pressure higher than 50 MPa. The $E_{sp\,cp}$ of Vivapur 12® is the highest, but the evolution is not linear. For compaction pressure higher than 150 MPa, $E_{sp\,cp}$ is almost constant. Between 0 and 70 MPa, the $E_{sp\,exp}$ values of the three single materials are nil. Above this compaction value, the $E_{sp\,exp}$ values increase. The most important increase is observed with Vivapur 12®.

Concerning the $E_{sp\,cp}$ of the binary mixtures, a linear fit describes well the change of the specific compaction energy with the mixture composition (w/w) at a constant compaction pressure (Fig. 4). This observation is assessed using the linearity test of likelihood ratios which corresponds to a Chi-square test. The linear fit is tested vs. a second degree polynomial fit with a number of degrees of freedom of 1

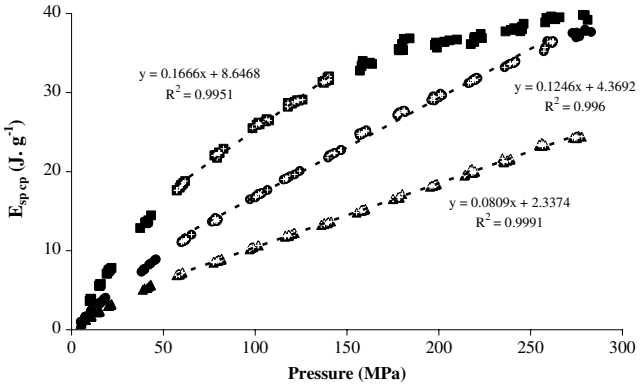


Fig. 2. Evolution of specific compaction energy ($E_{sp\,cp}$) versus compaction pressure. Key: ▲, A; ●, F; ■, V. The white crosses correspond to the linear evolution of $E_{sp\,cp}$.

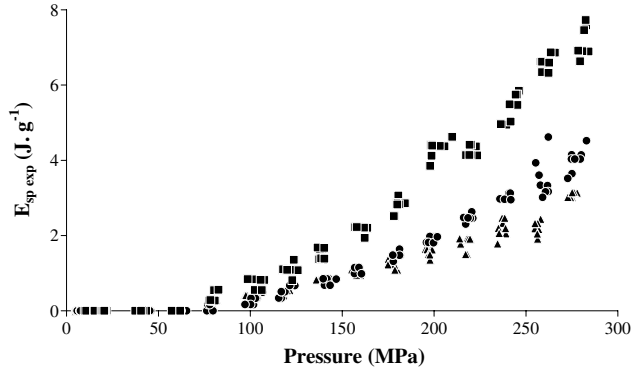


Fig. 3. Evolution of specific expansion energy ($E_{sp\,exp}$) versus compaction pressure. Key: ▲, A; ●, F; ■, V.

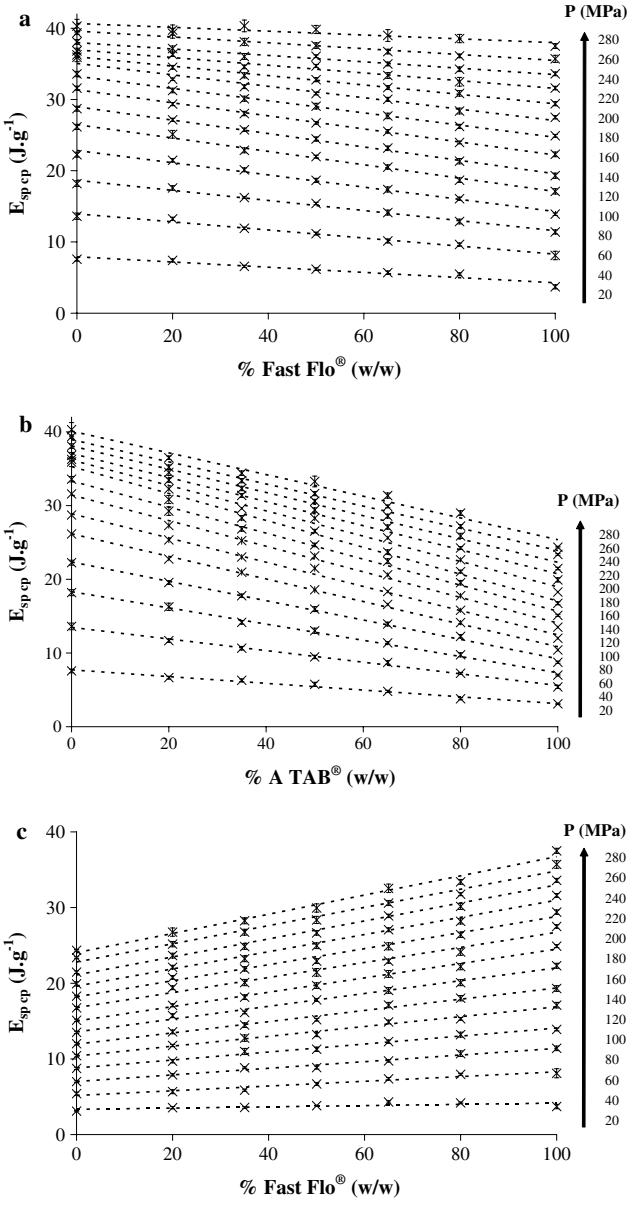


Fig. 4. Specific compaction energy ($E_{sp\,cp}$) of binary mixtures versus the mass composition, for different compaction pressures ($P$); $n = 8$; (a) Vivapur 12®/Fast Flo® mixtures (VF), (b) Vivapur 12®/A TAB® mixtures (VA), (c) A TAB®/Fast Flo® mixtures (AF).

and a risk of 5%. The test confirms that a linear relationship is more suitable in this case. Then, the following mixing rule can be used to calculate the specific compaction energy of a mixture from the data of the single materials:

$$E_{sp\,cp\,AB} = x \cdot E_{sp\,cp\,A} + (1 - x) \cdot E_{sp\,cp\,B}, \quad (3)$$

where $E_{sp\,cp\,A}$, $E_{sp\,cp\,B}$ and $E_{sp\,cp\,AB}$ are the specific compaction energies of the single components and their mixtures, respectively, $x$ and $(1 - x)$ are the weight fractions of the constituent powders.

For the VF mixtures, the change of $E_{sp\,cp}$ is limited, since the $E_{sp\,cp}$ values of the two single components are closer. For the AF and VA mixtures, the change is more

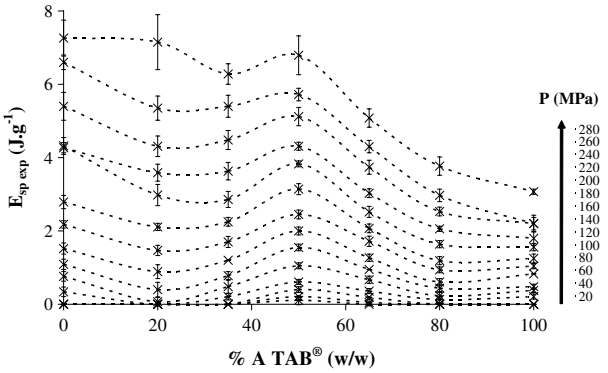


Fig. 5. Specific expansion energy ($E_{sp\ exp}$) of Vivapur 12®/A TAB® mixtures (VA) versus the mass composition of the mixture, for different compaction pressures ($P$); $n = 8$.

important, due to the higher $E_{sp\,cp}$ value of Vivapur 12® and Fast Flo®.

Contrary to $E_{sp\ cp}$, a linear fit is inappropriate to describe the change of $E_{sp\ exp}$ with the mass percentage of the mixture components. Fig. 5 shows the example of the VA mixtures. A TAB® and Fast Flo® are characterized by closer and lower $E_{sp\,exp}$ values. Then, $E_{sp\,exp}$ in the case of AF mixtures are almost constant for compaction pressures lower than 100 MPa (data not shown). Since Vivapur 12® is characterized by the highest values of $E_{sp\,exp}$, the mixtures with this excipient have an important specific energy of expansion too. The values of $E_{sp\,exp}$ of the VF and VA mixtures significantly decrease if the concentrations of A TAB® and Fast Flo® are higher than 50% (w/w) and 35% (w/w), respectively (see Fig. 5 with the example of VA mixtures).

Table 2 sums up the important energetic compressibility parameters of the single materials and the binary mixtures for a compaction pressure of 210 MPa.

### 3.3. Decrease of the porosity under pressure

The compressibility can be expressed by the decrease of the porosity under pressure. The compact porosities shown in Fig. 6 are calculated immediately after compaction from the weight, the size of the compacts and the apparent particular density. The porosities of the single-compound materials are shown by the closed symbols.

A TAB® has the lowest compressibility. For a range of pressure of 0–210 MPa, the porosity decrease is about 53% for A TAB®, whereas, it is more than 80% for the two other materials. This must be due to the fact that it deforms by fragmentation [11]. Due to its fragmenting behaviour, the densification of A TAB® is less important and it is linked with a limited range of porosity. For Vivapur 12® and Fast Flo®, when the applied pressure becomes higher than their mean yield pressures, the particles deform plastically and the porosity decrease is more important.

Table 2
Characteristic energies of the single-compound materials and the binary mixtures calculated from the compression cycles at 200 MPa on the Frogerais OA tabletting press ($n = 8$; values are expressed as means ± standard deviation)

| Notation | Specific compaction energy, $E_{sp\ cp}$ (J g$^{-1}$) | Specific expansion energy, $E_{sp\ exp}$ (J g$^{-1}$) |
|---|---|---|
| *V* | 36.3 ± 0.3 | 4.3 ± 0.2 |
| *A* | 18.3 ± 0.1 | 1.6 ± 0.1 |
| *F* | 29.4 ± 0.3 | 1.9 ± 0.1 |
| VF82 | 34.5 ± 0.3 | 4.0 ± 0.3 |
| VF63 | 33.4 ± 0.4 | 4.0 ± 0.2 |
| VF55 | 32.8 ± 0.3 | 3.1 ± 0.2 |
| VF36 | 31.7 ± 0.3 | 3.2 ± 0.2 |
| VF28 | 30.8 ± 0.4 | 3.1 ± 0.1 |
| VA82 | 32.3 ± 0.3 | 3.0 ± 0.3 |
| VA63 | 29.6 ± 0.2 | 2.9 ± 0.2 |
| VA55 | 29.4 ± 0.3 | 4.3 ± 0.1 |
| VA36 | 25.6 ± 0.2 | 2.5 ± 0.2 |
| VA28 | 22.6 ± 0.3 | 1.6 ± 0.1 |
| AF82 | 20.8 ± 0.2 | 1.4 ± 0.1 |
| AF63 | 21.9 ± 0.3 | 2.2 ± 0.2 |
| AF55 | 22.9 ± 0.3 | 2.1 ± 0.1 |
| AF36 | 24.9 ± 0.5 | 1.8 ± 0.1 |
| AF28 | 26.4 ± 0.4 | 2.5 ± 0.1 |

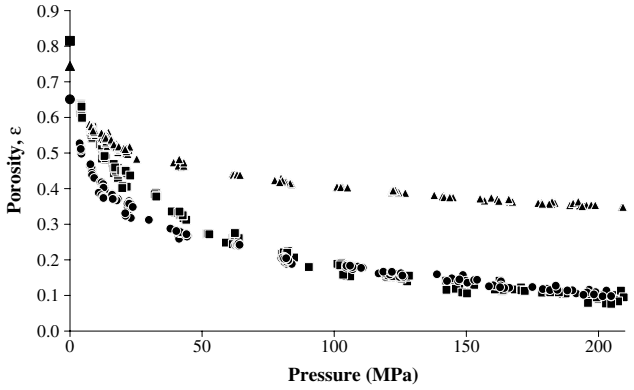


Fig. 6. Evolution of porosity of parallelepipedical compacts versus compaction pressure in the case of single materials. Key: ▲, A; ●, F; ■, V.

For the AF and VA mixtures, the ranges of porosities obtained are between those of the single materials. As previously observed by Larhrib and Wells [7,8], when the concentration of the brittle material (in this work, A TAB®) becomes higher, the range of porosity reduces. For example, the pressure needed to have a porosity of 20% increases. In the case of VA mixtures, this pressure is about 60 MPa for 80/20 (w/w) mixture and about 75 MPa for 65/35 (w/w) mixture compared to 56 MPa with Vivapur 12® powder. In the case of AF mixtures, this pressure is about 120 MPa for 20/80 (w/w) mixture and 160 MPa for 35/65 (w/w) mixture compared to 80 MPa with Fast Flo®. The particles of A TAB® which are brittle hinder the densification because these particles replace more plastic particles of Vivapur 12® or Fast Flo® that can fill more

easily the porosity. Bouvard [15] observed the same thing with the consolidation of a metal powder containing non-deformable inclusions. The author argued that since the applied pressure was not totally supported by the deformable matrix powder, a higher applied pressure had been exerted to the composite powder to obtain the same matrix density that could be achieved without inclusions. However, when the fraction of A TAB® is high, the densification is more controlled by the skeleton of A TAB® particles. In this situation, even with high pressures, the plastic deformation of Vivapur 12® and Fast Flo® particles is difficult or incomplete.

Concerning VF mixtures, the ranges of mixture porosities are very close to the porosities observed with Fast Flo® and Vivapur 12®, except for compaction pressure lower than 50 MPa.

More, it appears that for compaction pressures ranged between 20 and 200 MPa, the relationship between the porosity of the parallelepipedical compacts and the mixture composition (w/w) is linear (Figs. 7–9). This observation is in good accordance with the previous results of Ramaswamy et al. [16]. The porosity of a compacted mixture of two materials of equal particle sizes can then be easily calculated from the relationship porosity vs. pressure obtained with the single materials, i.e.:

$$\varepsilon_{AB} = x \cdot \varepsilon_A + (1 - x) \cdot \varepsilon_B, \quad (4)$$

where $\varepsilon_A$, $\varepsilon_B$ and $\varepsilon_{AB}$ are, respectively, the porosities of the parallelepipedical compacts composed of the single components and their mixtures at a same compaction pressure, $x$ and $(1 - x)$ are the weight fractions of the constituent powders.

In all the cases, the slope of the curve porosity vs. mixture composition increases with compaction pressure when it is below 120 MPa. For larger pressure levels, the slopes become a constant. This can be linked to the fact that this pressure is lower than the mean yield pressure of the most plastic material of the mixture.

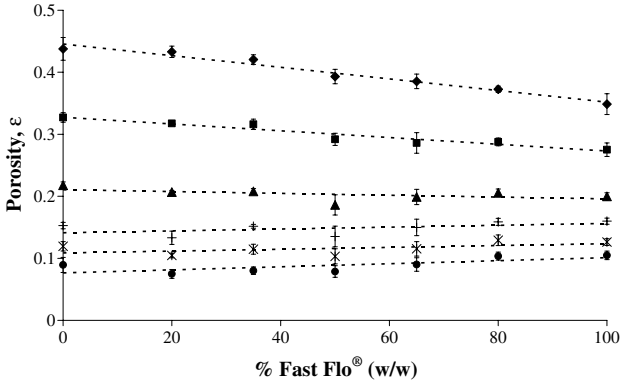


Fig. 7. Evolution of porosity of parallelepipedical compacts of Vivapur 12®/Fast Flo® (VF) mixtures at a constant compaction pressure. Key: ♦, 20 MPa, $y = -0.0009x + 0.4455$, $R^2 = 0.9686$; ■, 40 MPa, $y = -0.0005x + 0.3274$, $R^2 = 0.9212$; ▲, 80 MPa, $y = -0.0001x + 0.2106$, $R^2 = 0.2729$; +, 120 MPa, $y = 0.0002x + 0.1412$, $R^2 = 0.2143$; ∗, 160 MPa, $y = 0.0001x + 0.1086$, $R^2 = 0.2779$; ●, 200 MPa, $y = 0.0002x + 0.0765$, $R^2 = 0.5188$; $n = 10$.

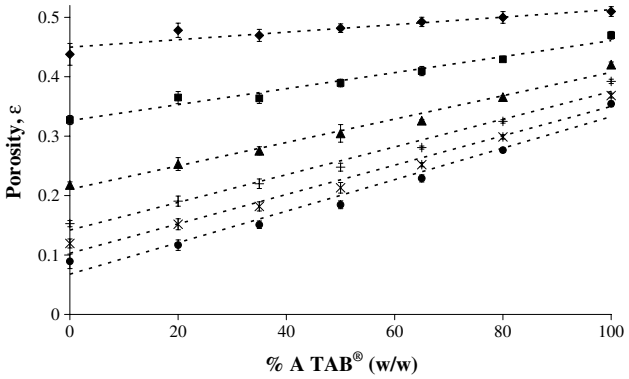


Fig. 8. Evolution of porosity of parallelepipedical compacts of Vivapur 12®/A TAB® (VA) mixtures at a constant compaction pressure. Key: ♦, 20 MPa, $y = 0.0006x + 0.4496$, $R^2 = 0.8754$; ■, 40 MPa, $y = 0.0013x + 0.3261$, $R^2 = 0.9726$; ▲, 80 MPa, $y = 0.0020x + 0.2106$, $R^2 = 0.9850$; +, 120 MPa, $y = 0.0023x + 0.1418$, $R^2 = 0.9821$; ∗, 160 MPa, $y = 0.0025x + 0.1029$, $R^2 = 0.9783$; ●, 200 MPa, $y = 0.0027x + 0.0676$, $R^2 = 0.9729$; $n = 10$.

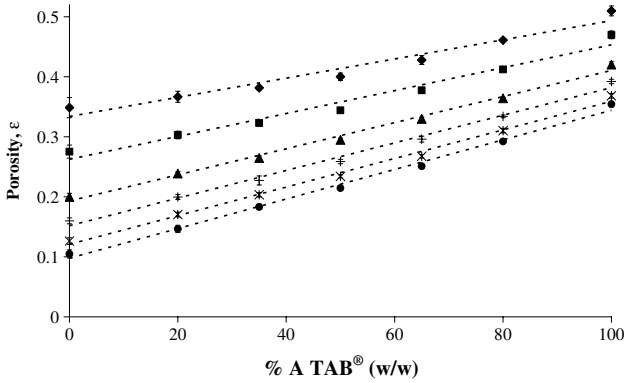


Fig. 9. Evolution of porosity of parallelepipedical compacts of A TAB®/Fast Flo® (AF) mixtures at a constant compaction pressure. Key: ♦, 20 MPa, $y = 0.0016x + 0.3338$, $R^2 = 0.9570$; ■, 40 MPa, $y = 0.0019x + 0.2625$, $R^2 = 0.9720$; ▲, 80 MPa, $y = 0.0022x + 0.1930$, $R^2 = 0.9929$; +, 120 MPa, $y = 0.0023x + 0.1518$, $R^2 = 0.9923$; ∗, 160 MPa, $y = 0.0024x + 0.1209$, $R^2 = 0.9946$; ●, 200 MPa, $y = 0.0025x + 0.0977$, $R^2 = 0.9943$; $n = 10$.

### 3.4. Heckel's plots

Compressibility of powder compacts is often studied using Heckel's plot, in the ($\varepsilon$, $P$) plane, where $\varepsilon$ is the compact porosity and $P$ is the applied pressure. The plots were generated from the compaction pressures and the relative density data collected during the compaction of the parallelepipedical compacts. Heckel assumed that the volume reduction of a plastically deforming particle bed was analogous to a first-order kinetics phenomenon, with the pores being the reactants and the densification of the bulk of the powder as products [17,18]. He then derived a linear relationship between the logarithm of the inverse of the sample porosity ($1/\varepsilon$) and the applied pressure ($P$):

$$\ln(1/\varepsilon) = k \cdot P + A, \quad (5)$$

where $k$ and $A$ are constants.

For pharmaceutical products, the plots are generally not linear on the whole range of pressure and a non-linear step corresponding to rearrangement and/or fragmentation is observed for the lowest pressure. From the linear portion of this curve, the parameter $k$ which has the dimension of an inverse of pressure is extracted and it is related to the plastic behaviour of the material. The mean yield pressure ($P_y$ in MPa) is defined by $1/k$. The $P_y$ can be obtained by the "in-die method" ($P_{yA}$) (i.e., under pressure) and by the "out-of-die method" ($P_{yB}$) (i.e., after totally elastic recovery of the compact) [19].

Heckel's plots obtained with the "in-die method" and the parallelepipedical compacts of the single materials appear in Figs. 10–12 (closed symbols). The plots of the three materials show a non-linear step corresponding to rearrangement and/or fragmentation for the lowest pressures. A linear curve that indicates plastic deformation is observed. The $P_{yA}$ values are calculated in the linear zone of the plot, between 40 and 100 MPa for Vivapur 12®, 50 and 210 MPa for Fast Flo®, 100 and 210 MPa for A TAB®. Three trials were performed for each component. The mean yield pressures of the single materials illustrate the difference in their densification behaviour. Vivapur 12® is a plastically deforming material [10], it is shown by its low mean yield pressure ($P_{yA} = 54 \pm 4$ MPa). A TAB® has a high mean yield pressure ($P_{yA} = 530 \pm 5$ MPa). As reported previously, it deforms by fragmentation [20] and due to its behaviour, it is linked with a limited range of porosity (see Fig. 6). With a $P_{yA}$ of $111 \pm 2$ MPa, Fast Flo® is an intermediate material. These values are lower than those obtained with the "out-of-die method" (Table 3). From $P_{yA}$ and $P_{yB}$, it is possible to calculate $P_{ye}$ ($1/P_{ye} = 1/P_{yA} - 1/P_{yB}$) which characterizes the tendency of a material to recover visco-elastically [19]. The lowest value of $P_{ye}$ is obtain with the Vivapur 12® compacts, whereas, A TAB® compacts show a little visco-elastic tendency (see Table 3).

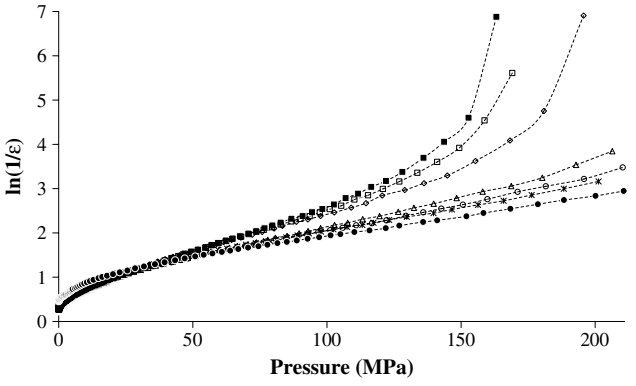


Fig. 10. Heckel's plots ("in-die" method) of Vivapur 12®/Fast Flo® (VF) mixtures in the case of parallelepipedical compacts. Key: ●, F; ■, V; □, VF82; ◇, VF63; △, VF55; ○, VF36; ∗, VF28.

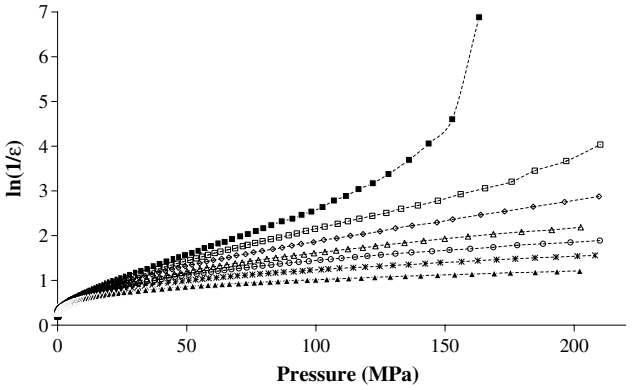


Fig. 11. Heckel's plots ("in-die" method) of Vivapur 12®/A TAB® (VA) mixtures in the case of parallelepipedical compacts. Key: ■, V; ▲, A; □, VA82; ◇, VA63; △, VA55; ○, VA36; ∗, VA28.

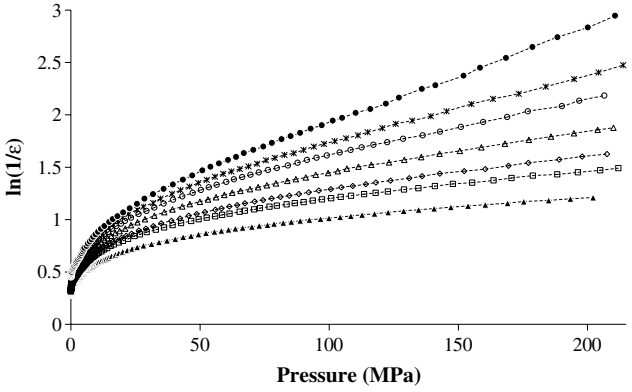


Fig. 12. Heckel's plots ("in-die" method) of A TAB®/Fast Flo® (AF) mixtures in the case of parallelepipedical compacts. Key: ▲, A; ●, F; □, AF82; ◇, AF63; △, AF55; ○, AF36; ∗, AF28.

Table 3
Mean yield pressures obtained from the Heckel's plot by "in-die" method ($P_{yA}$, $n = 3$) and by "out-of-die" method ($P_{yB}$) for the single-compound materials and the binary mixtures and $P_{ye}$ calculated using the following equation, $1/P_{ye} = 1/P_{yA} - 1/P_{yB}$

| Notation | $P_{yA}$ (MPa) | $P_{yB}$ (MPa) | $P_{ye}$ (MPa) |
|---|---|---|---|
| *V* | $54 \pm 4$ | 149 | 85 |
| *A* | $530 \pm 5$ | 714 | 2057 |
| *F* | $111 \pm 2$ | 189 | 269 |
| VF82 | $55 \pm 3$ | 131 | 95 |
| VF63 | $60 \pm 1$ | 145 | 102 |
| VF55 | $77 \pm 2$ | 154 | 154 |
| VF36 | $85 \pm 3$ | 161 | 180 |
| VF28 | $93 \pm 5$ | 178 | 195 |
| VA82 | $73 \pm 4$ | 169 | 129 |
| VA63 | $114 \pm 8$ | 204 | 258 |
| VA55 | $181 \pm 10$ | 294 | 471 |
| VA36 | $265 \pm 4$ | 333 | 1298 |
| VA28 | $378 \pm 6$ | 417 | 4042 |
| AF82 | $413 \pm 11$ | 555 | 1614 |
| AF63 | $322 \pm 10$ | 435 | 1240 |
| AF55 | $262 \pm 4$ | 385 | 820 |
| AF36 | $192 \pm 4$ | 333 | 453 |
| AF28 | $155 \pm 2$ | 250 | 408 |

The Fast Flo® value of $P_{ye}$ is in the same range as previous results obtained with some lactoses [9].

Heckel's plots for the mixtures demonstrate that all the mixtures behave like intermediate materials between the single materials (Figs. 10–12, opened symbols). In the case of VF mixtures, mixtures with 50–80% w/w of Fast Flo® seem to have a densification behaviour closer to those of Fast Flo®. When concentrations of Vivapur 12® are important, Heckel's plots are more similar to those of Vivapur 12®.

The relationships between the mean yield pressure obtained by the "in-die method" ($P_{yA}$) and mixture composition (w/w) are depicted in Fig. 13 (the values correspond to the average of three trials). For all the mixtures, the relationship between the $P_{yA}$ and the mixture composition is not linear. The compression behaviour of a mixture is not the weighted sum of the behaviour of the single components (dotted lines in Fig. 13) and the plots show a negative deviation from those predicted from the single materials. But, the negative deviation is limited in the case of VF mixtures, since the $P_{yA}$ values are closer. For VF mixtures, until 35% in mass of Fast Flo®, the $P_{yA}$ is controlled by Vivapur 12®. Between 35 and 50% w/w of Fast Flo®, the increase of $P_{yA}$ is more important. For higher concentrations, the $P_{yA}$ of the mixtures are closer to the $P_{yA}$ obtained by linear interpolation. In some previous studies, some authors have admitted that for products with close mean yield pressures, it is possible to predict linearly the compaction behaviour of the binary mixtures [5,6]. The $P_{yA}$ values for the mixtures of a plastically flowing material or an intermediate material with a fragmenting material show a more important negative deviation from the sum of the values of the single excipients. For the highest concentration of Vivapur 12® in VA mixtures (80% w/w and more), the densification depends on the behaviour of Vivapur 12®. From A TAB® concentrations of 65% (w/w), the mean yield pressure is no longer controlled by the Vivapur 12® particles since the $P_{yA}$ become higher than 250 MPa. A similar trend was observed by Ilka et al. [5] with microcrystalline cellulose and anhydrous calcium phosphate mixtures. On the contrary, Larhrib and Wells [7,8] give a positive deviation from a linear relationship for PEG/calcium phosphate (plastic/brittle) mixtures. For AF mixtures and for Fast Flo® concentrations higher than 65% w/w, $P_{yA}$ values below 200 MPa are observed. This can mean that the mixture behaviour is more controlled by Fast Flo®. A TAB® starts to control the $P_{yA}$ of the mixtures when Fast Flo® represents less than 50% in mass ($P_{yA}$ becomes higher than 250 MPa).

The values obtained with the "out-of-die method" ($P_{yB}$) are higher than those obtained with the "in-die method" ($P_{yA}$, Table 3), but the same trend is observed for the relationship between $P_{yB}$ and the mixture composition (w/w).

In the VA mixtures with more than 50% w/w of Vivapur 12®, the visco-elasticity tendency of the mixtures is important (see values of $P_{ye}$, Table 3). A similar trend is observed with AF mixtures. Otherwise, the increase of the A TAB® proportion in a mixture leads to a decrease of the visco-elasticity tendency. In the case of the VF mixtures, the change of $P_{ye}$ values is smaller since the $P_{ye}$ of the two single materials are closer.

### 3.5. Predictive approach for the mean yield pressure of the binary mixture

The results obtained show that the porosity of the compacted binary mixtures is proportional to the mixture composition (w/w), at a constant compaction pressure. It is then possible to calculate by a simple interpolation, at a constant pressure, the porosity of a compacted mixture from the data obtained with the single materials. If the compaction pressures belong to the linear zone of Heckel's plot, it is possible to draw this plot and to deduce the mean yield pressure of the mixture (Fig. 14):

$$\ln(1/\varepsilon_2) - \ln(1/\varepsilon_1) = k \cdot (P_2 - P_1), \quad (6)$$

where $\varepsilon_1$ and $\varepsilon_2$ are the porosities of the mixture compacted under the pressure $P_1$ and $P_2$.

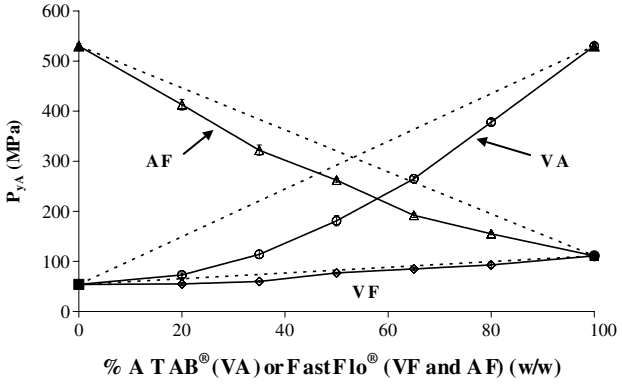


Fig. 13. Mean yield pressure ($P_{yA}$) obtained by the "in-die" method as a function of mass composition of the mixtures (parallelepipedical compacts). Key: ▲, A; ●, F; ■, V; ○, VA; ◇, VF; △, AF; $n = 3$. The dotted line represents the results of the use of a linear simple mixing rule.

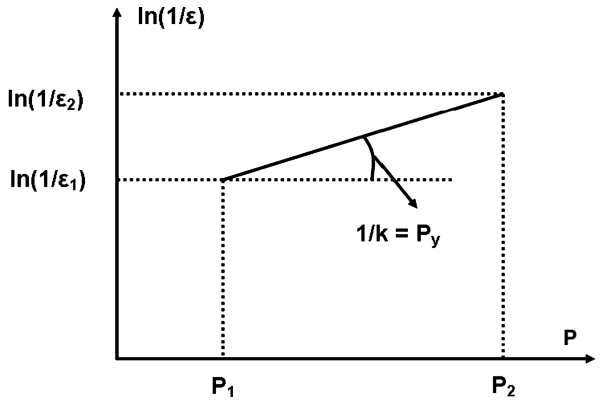


Fig. 14. Principle of the predictive approach for the mean yield pressure of a binary mixture.

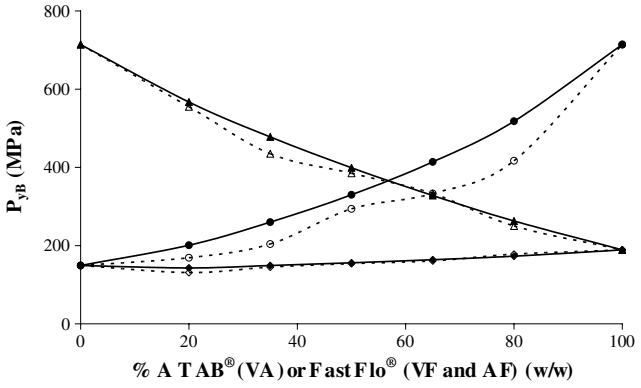


Fig. 15. Comparison between the experimental values of $P_{yB}$ (closed symbols) and the calculated values (opened symbols, Eq. (6)) vs. the mass composition of the mixtures. Key: ● and ○, VA mixtures; ♦ and ◇, VF mixtures; ▲ and △ AF mixtures.

In this work, for each mixture, $\varepsilon_1$ and $\varepsilon_2$ were calculated from the porosities of the single materials compacted under the pressure $P_1$ and $P_2$ using Eq. (4). In a second step, the mean yield pressure was obtained using Eq. (6). Since the porosities of the single materials were calculated after compaction (Eq. (2)), $\varepsilon_1$ and $\varepsilon_2$ are also the porosities of the compacted binary mixtures after compaction. The calculated mean yield pressure is then similar to a mean yield pressure obtained using the ''out-of-die method'', i.e. $P_{yB}$. The $P_{yB}$ values calculated with this predictive approach are very similar to the experimental values presented in Table 3 (Fig. 15). The most important variation is observed between the experimental and the predictive values with the VA mixtures.

The present approach can then be used to predict the mean yield pressure and the compaction behaviour of compacted binary mixtures simply from the properties of the single excipients.

## 4. Conclusion

In this work, the compressibility of some binary mixtures of pharmaceutical excipients with various mass concentrations was studied. Several approaches were used: compression cycles with energy measurements, decrease of the compact porosity under pressure and Heckel's plots. For the binary mixtures studied, it was observed that the specific compaction energy was proportional to the mixture composition expressed in mass. But, this was not the case for the specific expansion energy. Similarly for the specific compaction energy, a proportional relationship was observed between the compact porosity and the mass composition of the mixtures. Concerning the mean yield pressure, in all the cases, the relationship between the $P_y$ and the mixture composition was not linear and for the mixtures studied here, a negative deviation was observed. A predictive approach of the mean yield pressure based on the proportional relationship between porosity and mixture composition is proposed. The comparison of the calculated and experimental values proves the validity of this approach for various binary mixtures. It is then possible to predict the mean yield pressure of binary mixtures from the accessible data of the single excipients.

## References

[1] M. Duberg, C. Nystrom, Studies on direct compression of tablets. XII. The consolidation and bonding properties of some pharmaceutical compounds and their mixtures with Avicel 105, Int. J. Pharm. Technol. Prod. Mfr. 6 (2) (1985) 17–25.
[2] J.S.M. Garr, M.H. Rubinstein, The effect of rate of force application on the properties of microcrystalline cellulose and dibasic calcium phosphate mixtures, Int. J. Pharm. 73 (1991) 75–80.
[3] P. Humber-Droz, D. Mordier, E. Doelker, Densification behaviour of powder mixtures, Acta Pharm. Technol. 29 (1983) 69–73.
[4] M. Sheikh-Salem, J.T. Fell, Compaction characteristics of mixtures of materials with dissimilar compaction mechanisms, Int. J. Pharm. Tech. Prod. Mfr. 2 (1) (1981) 19–22.
[5] J. Ilkka, P. Paronen, Prediction of the compression behaviour of powder mixtures by the Heckel equation, Int. J. Pharm. 94 (1993) 181–187.
[6] B. Van Veen, K. Van der Voort Maarschalk, G.K. Bolhuis, K. Zuurman, H.W. Frijlink, Tensile strength of tablets containing two materials with a different compaction behaviour, Int. J. Pharm. 203 (2000) 71–79.
[7] H. Larhrib, J.I. Wells, Polyethylene glycol and dicalcium phosphate mixtures: effect of tabletting pressure, Int. J. Pharm. 159 (1997) 75–83.
[8] H. Larhrib, J.I. Wells, Compression speed on polyethylene glycol and dicalcium phosphate tableted mixtures, Int. J. Pharm. 160 (1998) 197–206.
[9] V. Busignies, P. Tchoreloff, B. Leclerc, M. Besnard, G. Couarraze, Compaction of crystallographic forms of pharmaceutical granular lactoses. I. Compressibility, Eur. J. Pharm. Biopharm. 58 (2004) 569–576.
[10] E. Doelker, Comparative compaction properties of various microcrystalline cellulose types and generic products, Drug. Dev. Ind. Pharm. 19 (1993) 2399–2471.
[11] C. Doldan, C. Souto, A. Concheiro, R. Martinez-Pacheco, J.L. Gomez-Amoza, Dicalcium phosphate dihydrate and anhydrous dicalcium phosphate for direct compression: a comparative study, Int. J. Pharm. 124 (1995) 69–74.
[12] T. Sebhatu, C. Ahlneck, G. Alderborn, The effect of moisture content on the compression and bond formation properties of amorphous lactose particles, Int. J. Pharm. 146 (1997) 101–114.
[13] C.-Y. Wu, S.M. Best, A.C. Bentham, B.C. Hancock, W. Bonfirld, A simple predictive model for the tensile strength of binary tablets, Eur. J. Pharm. Sci. 25 (2005) 331–336.
[14] C. Pontier, E. Champion, M. Viana, D. Chulia, D. Bernache-Assolant, Use of cycles of compression to characterize the behaviour of phosphate apatitic powders, J. Eur. Ceram. Soc. 22 (2002) 1205–1216.
[15] D. Bouvard, Densification behaviour of mixtures of hard and soft powders under pressure, Powder Technol. 111 (2000) 231–239.
[16] C.M. Ramaswamy, Y.B.G. Varma, D. Venkateswarlu, Compaction of mixtures of materials, Chem. Eng. J. 1 (1970) 168–171.
[17] W. Heckel, An analysis of powder compaction phenomena, Trans. Metallurg. Soc. AIME 221 (1961) 671–675.
[18] W. Heckel, Density–pressure relationship in powder compaction, Trans. Metallurg. Soc. AIME 221 (1961) 1001–1008.
[19] P. Paronen, M. Juslin, Compression characteristics of four starches, J. Pharm. Pharmacol. 35 (1983) 627–635.
[20] A. Munoz-Ruiz, T.P. Villar, N.M. Munoz, M.C.M. Perales, M.R.J. Castellanos, Analysis of the physical characterization and the tabletability of calcium phosphate-based materials, Int. J. Pharm. 110 (1994) 37–45.